Learning from the Optical Spectrum: Soft-Failure Identification and Localization [Invited]

Luis Velasco*, Behnam Shariati, Alba P. Vela, Jaume Comellas, and Marc Ruiz
Optical Communications Group (GCO), Universitat Politècnica de Catalunya (UPC), Barcelona, Spain
e-mail: lvelasco@ac.upc.edu

Abstract: The availability of coarse-resolution cost-effective Optical Spectrum Analyzers (OSA) allows its widespread deployment in operators' networks. In this paper, several machine learning approaches for failure identification and localization that take advantage of OSAs are presented.

OCIS codes: (060.0060) Fiber optics and optical communications, (060.1155) All optical networks

1. Introduction

Failure identification and localization can reduce failure repair times greatly. Failure localization techniques have been proposed mainly for hard failures, while significant work is still required for soft failure detection, identification, and localization. Note that some soft failures could affect signal QoT and eventually evolve to hard failures. In a recent work [1], the authors proposed monitoring the performance of lightpaths at the transponders side to verify their proper operation, as well as to detect BER degradations thus, anticipating connection disruptions. The authors analyzed several soft failure causes affecting signal QoT, such as *laser drift*, *filter shift*, and *tight filtering*, and propose algorithms to detect and identify the most probable failure. However, monitoring the signal at the egress node does not allow localizing failures and therefore, monitoring techniques to analyze and evaluate QoT in-line are required. In this regard, the availability of a new generation of cost-effective OSAs with sub-GHz resolution, integratable in the optical nodes [2], allows real-time monitoring of the optical spectrum of the lightpaths and computing their corresponding OSNR. Note that, when a signal is properly configured, its central frequency should be around the center of the assigned spectrum slot to avoid filtering effects, and it should be symmetrical with respect to its central frequency. Therefore, optical spectrum features can be exploited by machine learning-based algorithms to detect degradations and identify failures.

In this paper, we analyze DP-QPSK and 16QAM modulated signals and, from [4], study approaches to detect filtering related failures, i.e., *Filter Shift* and *Tight Filtering*; the optical spectrum would be asymmetrical in the case of filter shift, and its edges get noticeably rounded in the case of tight filtering. These changes allow distinguishing optical spectra suffering from such failures from properly configured ones. However, some of these effects, in particular for the case of tight filtering, can be observed when a properly configured signal passes through several filters (filter cascading). Therefore, it is of paramount importance to devise solutions to cope with this issue preventing the misclassification of a properly configured signal as a failed one. We study several alternatives solving this issue, which can be used individually or combined. Ultimately, the optical spectrum analysis can be used by sophisticated algorithms able to identify and localize failures. These algorithms can be deployed in the network controller, as well as in nodes' agents, close to the observation points, to reduce the amount of monitoring data to be conveyed to the control/management plane [3].

2. Failure detection and identification with OSAs

Let us firstly overview our proposed soft failure detection and identification process that utilizes the optical spectrums captured by OSAs deployed in the intermediate nodes [4]. The process involves both, modules running in node agents and modules running in the controller; this follows the architecture proposed in [3].

Fig. 1a shows an example of optical spectrum acquired by an OSA with 625 MHz resolution. In general, QPSK and 16QAM optical signals present, once filtered, a flat spectral region around the central frequency, sharp edges, and a round region between the edges and the central one. Running in node agents, a module named as Feature Extraction (FeX) receives the C-band optical spectrum acquired by the local OSA and extracts the data for the portion of the spectrum allocated to the lightpath under study; data consists of an ordered list of frequency-power (<*f*, *p*>) pairs. After equalizing power, so the maximum power to be 0 dBm, the derivative of the power with respect to the frequency is computed; Fig. 1b illustrates the derivative of the example optical signal, where sharp convexity can be observed close to the edges. Next, the FeX module characterizes the mean (μ) and the standard deviation (σ) of the power around the central frequency ($fc \pm \Delta f$), as well as a set of primary features computed as cut-off points of the signal with the following power levels: *i*) equalized noise level, denoted as *sig* (e.g., -60dB + equalization level); *ii*) edges of the signal computed using the derivative, denoted as $\hat{\partial}$; *iii*) a family of power levels computed w.r.t. μ-$k\sigma$, denoted as $k\sigma$; and *iv*) a family of power levels computed with respect to μ-*m*dB, denoted as -*mdB*. Each of these power levels generates a couple of cut-off

The research leading to these results has received funding from the EC through the METRO-HAUL project (G.A. nº 761727), from the Spanish MINECO TWINS project (TEC2017-90097-R), and from the Catalan Institution for Research and Advanced Studies (ICREA).

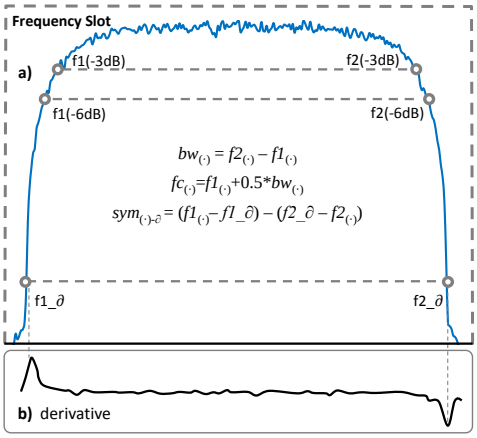

Fig. 1. Relevant points of a QPSK modulated signal

points denoted as $f1_{(\cdot)}$ and $f2_{(\cdot)}$. In addition, the assigned frequency slot is denoted as $f1_{slot}$, $f2_{slot}$. Other features are computed as linear combinations of the relevant point focus on characterizing a given optical signal (see embedded equations in Fig. 1a); they include: bandwidth (*bw*), central frequency (*fc*), and symmetry (*sym*) with respect to a reference (frequency slot or derivatives). Some features are more appropriate for filter related failure identification, such as bandwidth and symmetry at -3dB and -6dB, whereas other features, such as the central frequency, are more appropriate for laser drift identification.

After features have been extracted from the optical signal, a classification module named as Signal Spectrum Verification (SSV) running also in the node agents analyzes those features to detect a misconfiguration. The SSV module was implemented as a multiclass classifier in the form of a decision tree that produces a diagnosis which consists of *i*) a predicted class among the following options: '*Normal*', '*LaserDrift*', '*FilterFailure*'; and *ii*) a subset of relevant signal points for the predicted class. In the case that a filter failure is detected, another classifier is used to predict whether the failure is due to *FilterShift* or *TightFiltering*. The decision-making units of this secondary classifier are realized as support vector machine (SVM) binary classifiers exploiting i^{th} order polynomials as kernel function [5].

Finally, the FailurE causE Localization for optIcal NetworkinG (FEELING) algorithm running in the network controller commands the classification modules. One of the key challenges in the identification of filter related failures is the misclassification of a normal signal that has passed through several filters (i.e., affected by filter cascading) as a signal which has suffered from filter failures. Therefore, to improve failure identification accuracy, the FEELING algorithm must be able to distinguish between actual failures and normal effects arising from filter cascading. In the next section, we propose three alternatives to prevent such misclassification. Furthermore, since filter failures have impact on the OSNR, we take advantage of OSNR computation in intermediate nodes from the optical acquired signal to complement and enhance FEELING failure localization.

3. Approaches for optical spectrum analysis and signal classification

When a normal signal passes through several filters, it becomes narrower; the higher the number of the filters, the narrower the signal. As a result of filter cascading, signal features change in a similar way it happens when a tight filtering failure takes place.

The most straightforward solution to circumvent this issue is to correct feature values of a signal which is acquired after passing *N* filters, by adding/subtracting the differences w.r.t. feature values of the signal acquired in the ingress node (just after the transponder); we call such process as *correction mask*. This approach is conceptually shown in Fig. 2a. The correction mask can be computed a priori, assuming the changes a normal signal experiences while passing through different number of WSSs. Considering this approach, a single classifier can be trained based on the observations of the signal in the ingress node, where the impact of filter cascading is negligible, and it can be used at every intermediate node. A different approach that does not need correcting signal features is shown in Fig. 2b; it uses differentiated classifiers trained based on the observations collected from signals after passing through a specific number of WSSs. The complete set of classifiers needs to be available in every intermediate node and the appropriate one is used when a new signal spectrum is received. In the previous approaches, we aimed at avoiding the filter cascading problem either by correcting the computed features or by exploiting multiple classifiers on unaltered signal features. An alternative approach is to compare the received signal against the *expected signal* after a given number of filters. The expected signal at the ingress node can be obtained theoretically, whereas expected signals after a number of WSSs can be obtained assuming a certain transfer function for the filters, e.g., 2nd order Gaussian. In this approach, a classifier needs to be trained to work on the residuals resulting from computing the difference between acquired and expected signal spectra.

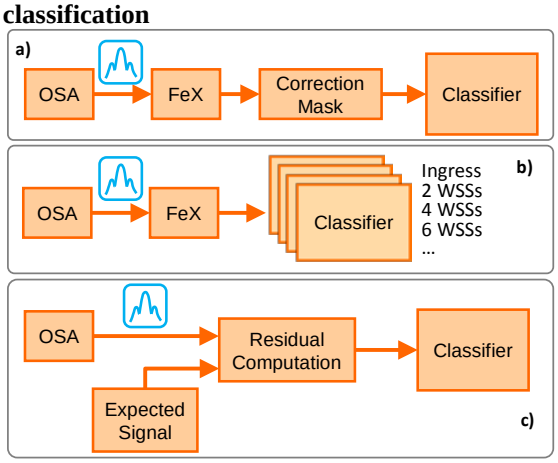

Fig. 2. Approaches to solve the filter cascading problem: a) correction mask, b) multi-classifier, and c) residual computation.

4. Results for the three approaches

In this section, we discuss a set of results showing how different approaches cope with the filter cascading problem. To this end, we configured a VPIPhotonics scenario where we emulate independently a 100 Gb/s DP-QPSK and a 200 GB/s 16QAM modulated signals. In the transmitter side, the optical signal is generated and it

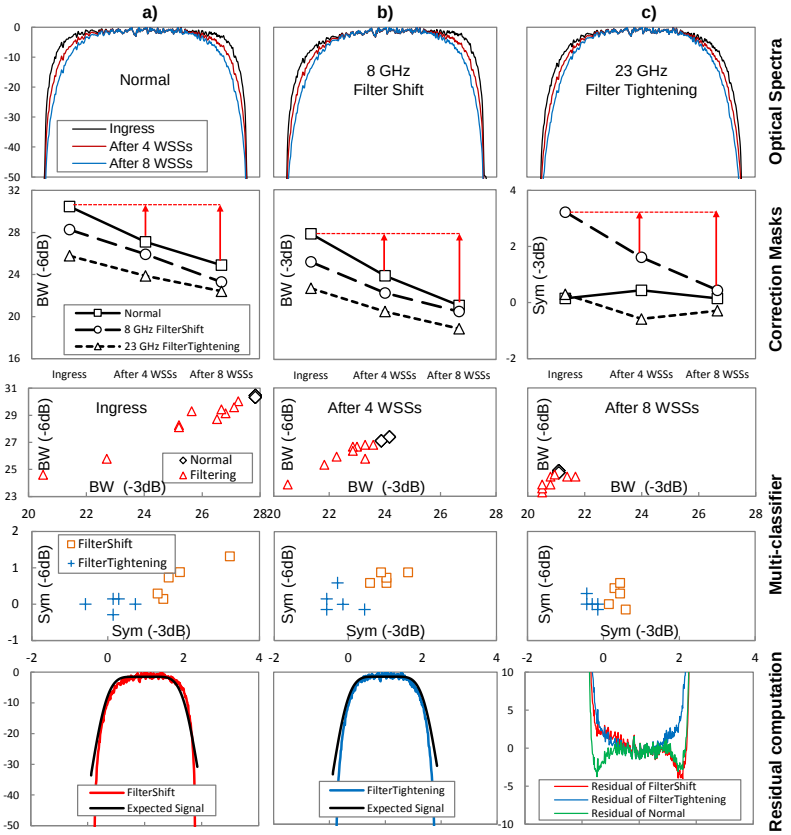

Fig. 3. Results for the considered approaches to solve the filter cascading problem.

passes through several fiber spans. After each span, an optical amplifier compensates for the accumulated attenuation of the fiber. Every optical node is considered to have two WSSs, where each one of them is modeled as a single optical filter with a 2nd order Gaussian transfer function; filters bandwidth is set to 37.5 GHz, leaving 7.5 GHz as a guard band for the lightpath. Finally, the optical signal ends in a coherent receiver that compensates for the impairments introduced throughout the transmission. In addition, 625 MHz OSAs are placed after every optical node to analyze the optical spectrum. Although in the following we present the obtained results for the DP-QPSK signal, they are valid for the 16QAM signal, since their spectra look almost identical after normalization.

Fig. 3 presents the results. The figure is divided into rows with the acquired optical spectrum on the first row and with the results for the three different approaches defined in the previous section. Regarding the acquired signal spectra, three graphs present a normal signal, another affected by 8 GHz filter shift, and a third affected by 23 GHz tight filtering. Each graph plots three spectra for the signal acquired in the ingress, after 4 WSSs and after 8 WSSs.

For the first approach (i.e., *Correction Masks*), the key signal features need to be corrected to compensate filter cascading. Fig. 3 shows the evolution of three key features (i.e., $bw_{(-3dB)}$, $bw_{(-6dB)}$, $sym_{(-3dB)\text{-}\partial}$) used for the classification purposes; the features should be corrected as shown by the red arrows in the figures. After such correction is applied, the single classifier trained based on the observations collected after the ingress node can perfectly distinguish filter related failures after any number of WSSs (up to 10 WSSs have been tested). For the multi-classifier approach, Fig. 3 plots $bw_{(-6dB)}$ and $sym_{(-3dB)\text{-}\partial}$ against $bw_{(-3dB)}$ and $sym_{(-3dB)\text{-}\partial}$; the plots allow SVMs to differentiate among *Normal*, *FilterShift*, and *TightFiltering* classes. Although classifiers provide accuracy higher than 95%, as the number of WSSs increases more complex SVM models are required. For instance, while at the ingress node a linear kernel and three support vectors are enough to achieve 95% accuracy, the classifier responsible for the classification after 8 WSSs, requires a 2nd order polynomial kernel and 6 support vectors to achieve 95% accuracy. Finally, for the residual computation approach, Fig. 3 presents acquired and expected signals after 4 WSSs for the filter shift and filter tightening failures, as well as the residuals calculated by subtracting actual and expected signals. As shown, the residuals for the filter shift failure look completely different from for the tight filtering problem; these shapes change also based on the magnitude of the failures. Therefore, a classifier can be developed fed by features computed on the residuals.

Even though these approaches enhance the accuracy of FEELING to cope with the filter cascading problem, the captured OSNR values can be additionally used for failure localization. Fig. 4 shows the measured OSNR evolution for three signals: normal signal, a signal affected by filter shift after node 2 (N2), and a signal affected by filter shift after N4. While the normal signal follows a smooth trend from N1 to N4, the slope of the trend of the signal affected by a filter shift changes after a particular node, which reveals the location of the failure.

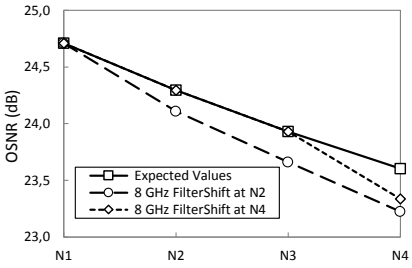

Fig. 4. OSNR degradation due to failures

References

[1] A. P. Vela et al., "BER Degradation Detection and Failure Identification in Elastic Optical Networks," IEEE/OSA JLT, 2017.
[2] Finisar. Flexgrid High Resolution Optical Channel Monitor (OCM) [On-line] www.finisar.com, 2017.
[3] A. P. Vela et al., "Distributing Data Analytics for Efficient Multiple Traffic Anomalies Detection," Elsevier Comp. Comm., 2017.
[4] A. P. Vela et al., "Soft Failure Localization during Commissioning Testing and Lightpath Operation," IEEE/OSA JOCN, 2018
[5] C. Bishop, Pattern Recognition and Machine Learning, Springer-Verlag, 2006.